



MECH 4402 – Simulation Tools for Design & Analysis

Date - December 10th, 2023

Final Report

Table of Contents

1.0 Summary	3
2.0 Introduction	3
3.0 Methodology	4
4.0 Results.....	6
4.1 Finite Element Analysis (FEA) Simulations	6
4.1.1 Hull FEA simulations	6
4.1.2 Backward End Cap FEA simulations	8
4.1.3 Forward End Cap FEA simulations.....	9
4.1.4 Interface Rings FEA simulation.....	10
4.2 Computational Fluid Dynamics (CFD) Analysis.....	11
4.2.1 CFD Analysis in XY-axis	11
4.2.2 CFD YZ-axis analysis.....	12
5.0 Summary and Conclusion	13
6.0 Contribution Statements.....	14
7.0 References	14
Appendix.....	15
CFD Analysis in XY-axis.....	15
CFD YZ-axis analysis.....	20

1.0 Summary

During the course of the project, the main goal was to achieve the project requirements for the achievable diving depth of the Titan submarine without experiencing structural failure, the structural integrity analysis of the individual parts (hull, interface rings and the caps), factor of safety, and to design structural improvements using Computational Fluid Dynamics (referred to CFD) analysis and Finite Element Analysis (referred to FEA) simulation, with the software Siemens Star CCM+ and Solidworks was used. Initially, a simplified submarine design (Figure 1) was tested for FEA simulation with titanium alloy and carbon fiber [1] materialistic properties on a trial-and-error basis. From the initial dimensions of the Titan, the improvements to our designs ensured the wall thickness was constant throughout which enabled the design to reduce the structural fatigue in the body design. With the end caps initially having a thickness of 83mm [2], the final design had a reduced thickness of 50 mm. In addition, from the FEA simulation of the final design, the hull of the submarine achieved a diving depth of 12.348 km withstanding a water pressure of 1.24E5 kPa with the carbon fiber hull (refer to section 4.1.1). Using CFD analysis, the hydrodynamic resistance of the Titan was calculated (refer to section 4.2).

2.0 Introduction

The main goal of this report was to learn and focus on the engineering analysis of the Titan, mostly on the design and material that was used to create the vessel at which point did it lead to the catastrophic implosion during the mission to voyage to the Titanic wreckage. With the severity of the incident, it fell upon the responsibilities of the engineers in charge of constructing the Titan, to ensure the design and material selection met the standards which it required to dive such depths. Following the strategy applied to Fossett's *DeepFlight Challenger*, the Titan was based on the same estimates [2].

For our project analysis, the submarine was simplified (Figure 1) into four components: Hull, Interface Rings, Backward End Cap, and Forward End Cap with a window cutout for an acrylic window of 380 mm in diameter and conical frustum shape of 180mm thick. With the dimensions of the Titan of 670 cm * 280 cm * 250cm, there was little room for error when designing, and all the components needed to be precise and within tolerance. The titanium end caps were bolted to the titanium rings, where the rings were bonded to the hull, made of carbon fiber wound, at both ends, and the forward end cap acted as an entrance and exit for the crew members. However, the Titan's features also present potential vulnerabilities, particularly at deeper depths of the ocean where conditions are extreme. Under immense pressure at the depths Titan operates, the slightest compromise in any of these components could lead to catastrophic consequences. If the pressure is not evenly distributed or if there's a flaw in the connection of the interface caps or bolts, it could become a focal point for structural failure. Any irregularities in the window or its connection could be a source of weakness, potentially leading to structural vulnerabilities. In the case of the hull, the winding process of the carbon fiber-wound material introduces the possibility of imperfections or weaknesses in the overall structural integrity of the hull.

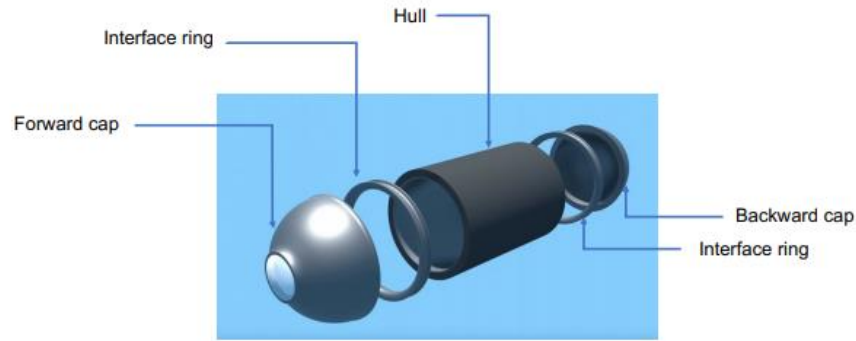


Figure 1: Simplified version of the Titan

During the modeling and the analysis process within the scope of the project, it was a challenge to estimate a fixed loading point in the FEA simulation. Since the water pressure acted on all sides while submerged, we had to assume a fixed point. Furthermore, the FEA simulation was done for individual parts to gauge the failing depth of each part, rather than in an assembly. Doing so increased the simulation time but gave an accurate analysis leading to maximum failure depth as required for the project milestone. Additionally, using Star CCM+, a virtual domain was created to test and analyze the hydrodynamic resistance encountered by the Titan maneuvering through various directions. The desired pressure and max velocity were calculated at different depths using CFD analysis and the factor of safety and achievable depths before failure was calculated from the FEA simulation.

3.0 Methodology

For the design project approach, we needed to estimate the maximum achievable depth that the Titan can dive without structural failure. From the project description with the given geometry, the Titan reached a speed of 3 knots (equal to 5.6 km/h or 3.5 mph) by utilizing a set of four electric thrusters, with the steering controls operated by a Logitech F710 wireless game controller. With the Titan comprising several bolted and bonded structures and components, under immense pressure and water temperatures, the slightest compromise in the structural body led it to implode in on itself at 3800m [2].

For the CFD simulations part of the project, the material used for fluid flow was *liquid*, mainly salt water mimicking real-life conditions, with a *constant density* and *constant dynamic viscosity* of 1023.6 kg/m^3 and $8.887\text{E-}4 \text{ Pa.s}$ respectively. In engineering, it is extremely difficult to simulate a real-life scenario. A certain set of assumptions are made to simplify the problem and simulation. The first assumption is the system is at a *steady-state* time interval. Secondly, the flow is *coupled with implicit flow* with the flow in a *turbulent regime*. The boundary conditions associated with the simulations were that the top and bottom wall surface of the domain was slip condition whereas the wall of the submarine subtract was no slip, with the inlet set as the speed of the Titan. The solvers and models used for the simulation *K-Epsilon turbulence*, *three dimensional*, *Reynolds-Averaged Navier Stokes equations*, *Realizable K-Epsilon Two-Layer*, *Two-Layer All y+ wall treatment and wall distance*. Since it was a 3D simulation, the 3D automated mesh was used with trimmed cell and prism layer mesher respectively. In addition, numerous mesh element sizes were used ranging from coarse to fine (1.0m to 0.05m), other parameters such as prism layer near wall thickness at 0.001 m, prism layer total thickness of 33.33 relative to base, target surface size 10 relative to base, minimum surface size 10 relative to base and number of prism layers of 2 were kept constant.

For the FEA simulations part of the project, the material for the interface rings, forward end cap, and backward end cap was Titanium (Ti), with set defined materialistic properties of mass density, Poisson's ratio, Young's modulus, and Yield Strength of 4600 kg/m³, 0.3, 1.1E11 Pa and 1.4E8 Pa respectively. In the case of the hull, the material used was carbon fiber [1], with set-defined materialistic properties of mass density, Poisson's ratio, Young's modulus, and Yield Strength of 1.41E9 kg/m³, 0.286, 9.94E10 Pa and 1.22E9 Pa respectively. To simplify the problem and simulation an assumption of linear elastic properties was used for the solver and models, as well as solid stress, at steady state. In addition, numerous mesh quality ranging from coarse to fine mesher was used.

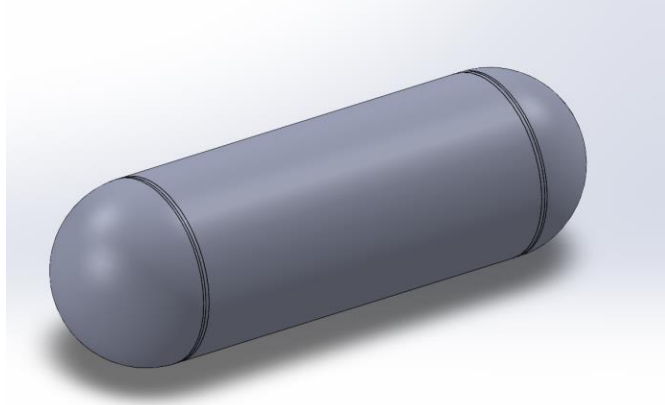


Figure 2: Simplified Geometry of Submarine Hull for CFD

As shown in Figure 2, the hull's window was removed for flow analysis in Star CCM+ for CFD analysis. The following simplification resulted in a symmetrical geometry that only requires simulations in two scenarios instead of four. For the first case, the flow was along the x-axis and y-axis as shown in Figures 3 and 4 respectively. The length of the capsule shape was 538.6 cm with a diameter of 168 cm.

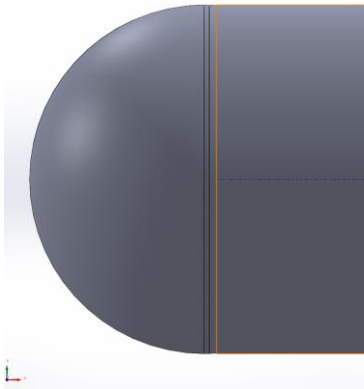


Figure 3: Flow Simulation along the X-axis

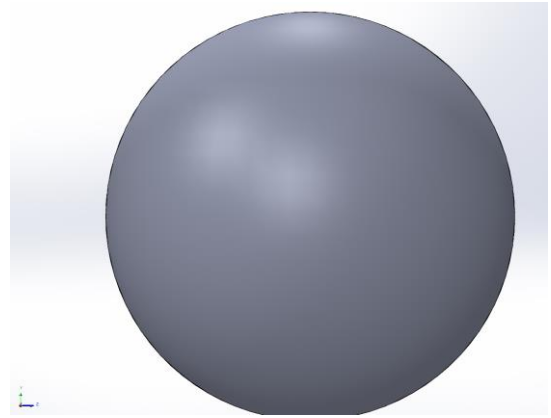


Figure 4: Flow Simulation along the Y-axis

Reynold's number is a unitless entity to indicate the flow regime of an object in a moving fluid. For an external flow over this capsule shape is:

$$Re = \frac{\rho U D}{\mu} = 3.0108E6 > 20,000$$

Equation 1: External Flow Reynolds number

Where:

ρ = Density of salt water = 1023.6 kg/m³
 U = Freestream velocity 3 knots = 1.556 m/s
 D = Diameter of capsule = 1.68 m
 μ = Dynamic viscosity of water = 8.8871E-4 Pa.s

From equation 1, the external flow around an obstacle is at critical Reynold's number of 20,000 or greater which in our case is satisfied. The coefficient of drag of the shape is approximately 0.7 from Figure 5, given the length ($L=538.6$ cm) and height ($H=168$ cm) resulting in an L/H ratio of 3.2.

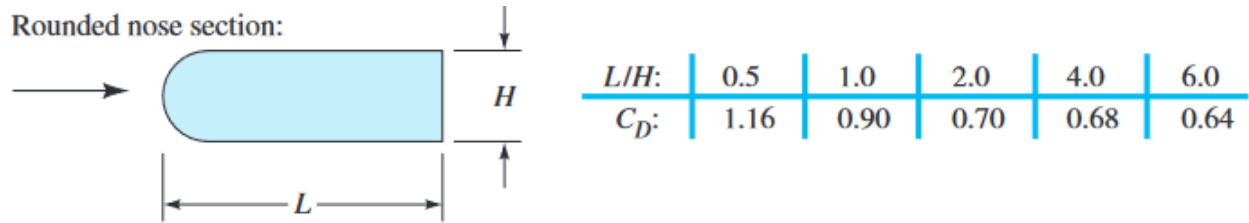


Figure 5: Capsule's Coefficient of drag

4.0 Results

For achieving the project milestones, the maximum depth for structural failure, the structural integrity analysis of the individual parts (hull, interface rings, and the caps), a factor of safety, and structural improvements were conducted using the software Siemens Star CCM+ and Solidworks. Several iterations were done at different ocean depths with varying pressure to precisely analyze the effect on the Titan.

4.1 Finite Element Analysis (FEA) Simulations

Numerous iterations have been conducted with varying depths and pressure acting on the individual parts of the Titan submarine to determine the point of structural failure. Equation 2 is used to calculate the factor of safety (FOS) for each of the parts from the simulation.

$$\text{Factor of safety (FOS)} = \frac{\text{Yield Strength}}{\text{Maximum Von Mises Stress}}$$

Equation 2: Factor of safety equation

Along with the factor of safety, the water pressure at each depth is calculated using equation 3, where ρ = Density of salt water = 1023.6 kg/m³, g = Acceleration due to gravity = 9.81 m/s² and h = Height of the fluid column = (m).

$$P = \rho gh$$

Equation 3: Hydrostatic water pressure

4.1.1 Hull FEA simulations

In the case of the hull, the material used was carbon fiber [1], with set-defined materialistic properties of mass density, Poisson's ratio, Young's modulus, and Yield Strength of 1.41E9 kg/m³, 0.286, 9.94E10 Pa and 1.22E9 Pa respectively, along with a wall thickness of 260 mm. Table 1 displays the parameters for the hull at varying boundary conditions for the figure number from the reports obtained from the FEA simulation.

Table 1: Parameter values for Hull FEA analysis

Figure Number	Ocean Depth (m)	Water Pressure (kPa)	Maximum Von Mises Stress (Pa)	Factor of Safety (FOS)
6	950	9536.18	9.501E7	12.84
7	1900	19072.37	1.897E8	6.43
8	3800	38144.73	3.793E8	3.22
9	12348	12400038144.73	1.233E9	0.99

From the tabulated results in table 1, at the ocean depth of 3800 m, at the Titanic depth, the hull of the Titan had a factor of safety of 3.22. Figure 8 exhibits the stress acting on the hull and where it possibly might lead to structural failure. In addition, it can be seen that at a depth of 12348 m, the hull of the Titan begins to weaken in its structural strength and ends up failing.

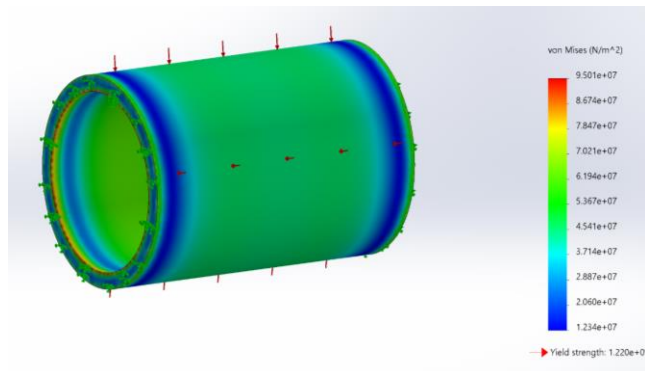


Figure 6: Hull at a depth of 950 m

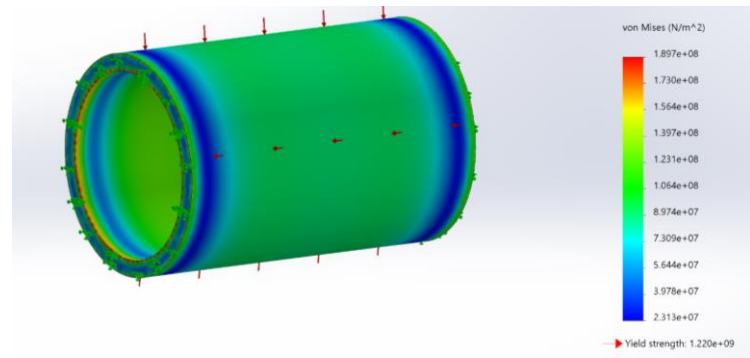


Figure 7: Hull at a depth of 1900 m

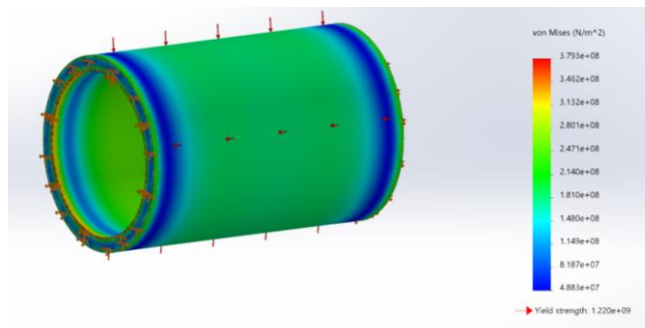


Figure 8: Hull at a depth of 3800 m

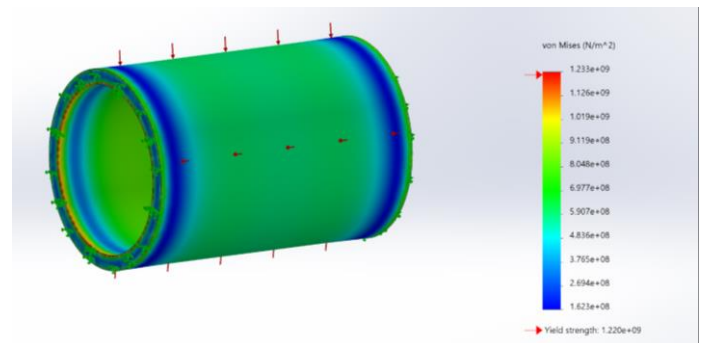


Figure 9: Hull at a depth of 12348 m

4.1.2 Backward End Cap FEA simulations

In the case of the backward end cap, the material used was Titanium (Ti), with set defined materialistic properties of mass density, Poisson's ratio, Young's modulus, and Yield Strength of 4600 kg/m³, 0.3, 1.1E11

Pa and 1.4E8 Pa respectively. Table 2 displays the parameters for the end cap at varying boundary conditions for the figure number from the reports obtained from the FEA simulation.

Table 2: Parameter values for Backward End Cap FEA analysis

Figure Number	Ocean Depth (m)	Wall Thickness (mm)	Water Pressure (kPa)	Maximum Von Mises Stress (Pa)	Factor of Safety (FOS)
10	3800	83	38144.73	3.325E7	4.21
11	3800	50	38144.73	3.242E7	4.32
12	16730	83	168000	1.464E8	0.96

Comparing figure 10 and 11, except the wall thickness, variables such as the ocean depth and water pressure are kept constant to examine the effect on the maximum Von Mises Stress and the Factor of Safety. The decrease in the end cap wall thickness increases the factor of safety slightly but further decreasing will have the opposite effect with reducing the factor of safety. Figure 12 exhibits the structural failure point of the backward end cap at a thickness of 83 mm and depth of 16730 m.

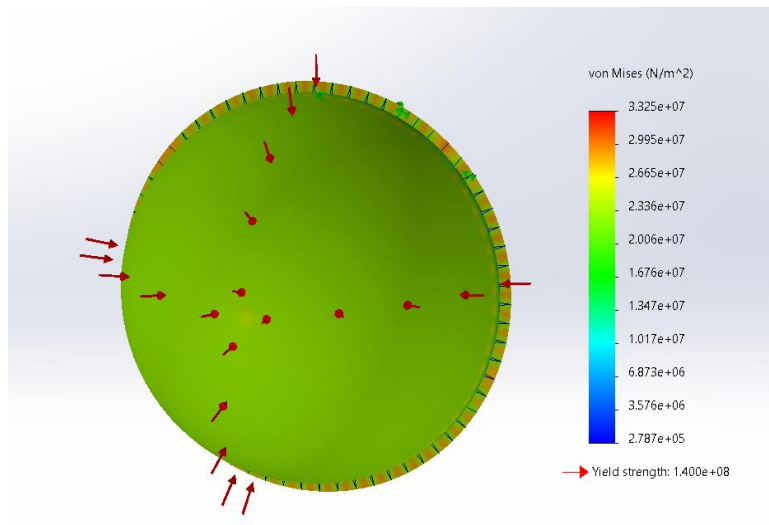


Figure 10: Backward End Cap at a depth of 3800 m at 83 mm thickness

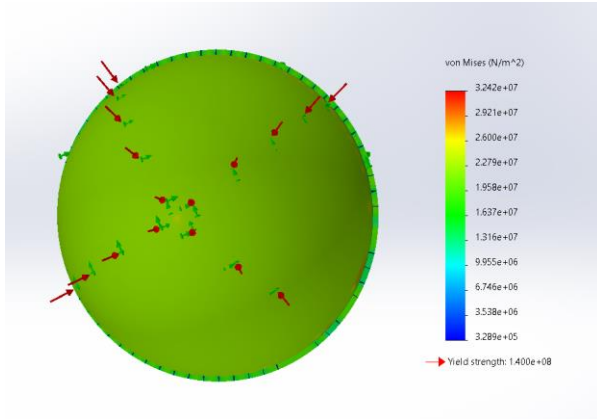


Figure 11: Backward End Cap at a depth of 3800 m at 50 mm thickness

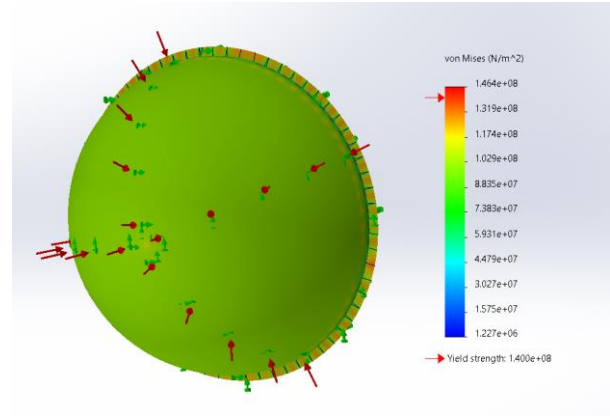


Figure 12: Backward End Cap at a depth of 16730 m at 83 mm thickness

4.1.3 Forward End Cap FEA simulations

In the case of the forward end cap, the material used was Titanium (Ti), with set defined materialistic properties of mass density, Poisson's ratio, Young's modulus, and Yield Strength of 4600 kg/m^3 , 0.3, $1.1\text{E}11 \text{ Pa}$ and $1.4\text{E}8 \text{ Pa}$ respectively. Table 3 displays the parameters for the end cap at varying boundary conditions for the figure number from the reports obtained from the FEA simulation.

Table 3: Parameter values for Forward End Cap FEA analysis

Figure Number	Ocean Depth (m)	Wall Thickness (mm)	Water Pressure (kPa)	Maximum Von Mises Stress (Pa)	Factor of Safety (FOS)
13	3800	83	38144.73	4.284E7	3.27
14	3800	60	38144.73	3.895E7	3.59
15	16740	83	136000	1.527E8	0.92

Comparing figure 13 and 14, except the wall thickness, variables such as the ocean depth and water pressure are kept constant to examine the effect on the maximum Von Mises Stress and the Factor of Safety. The decrease in the end cap wall thickness increases the factor of safety slightly but further decreasing will have the opposite effect with reducing the factor of safety. Figure 15 exhibits the structural failure point of the backward end cap at a thickness of 83 mm and depth of 16740 m.

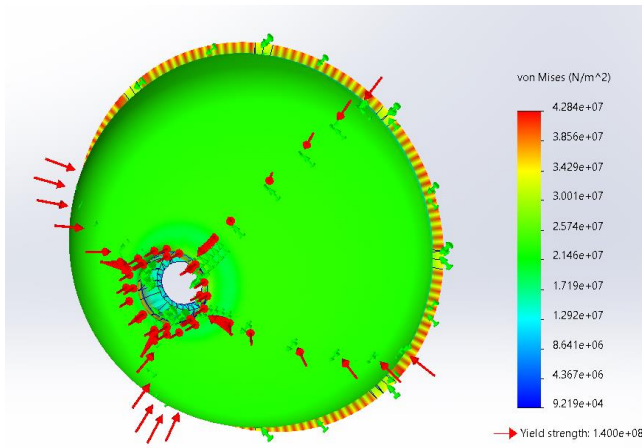


Figure 13: Forward End Cap at a depth of 3800 m at 83 mm thickness

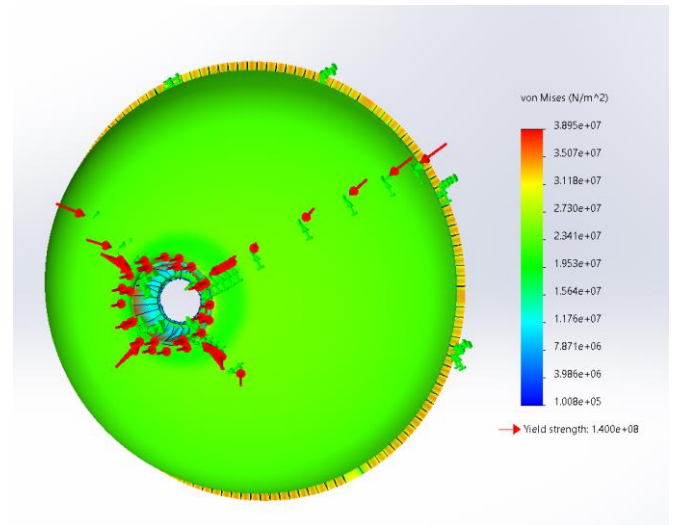


Figure 14: Forward End Cap at a depth of 3800 m at 60 mm thickness

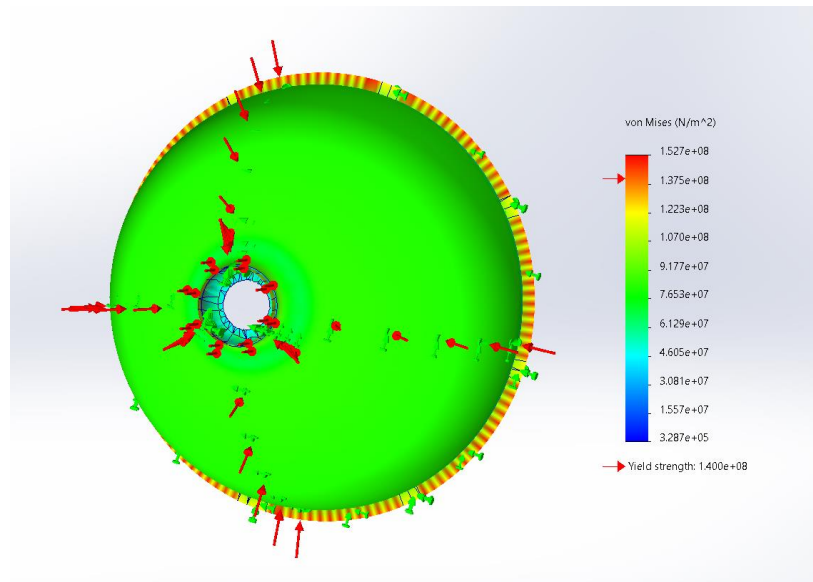


Figure 15: Forward End Cap at a depth of 16740 m at 83 mm thickness

4.1.4 Interface Rings FEA simulation

In the case of the interface rings, the material used was Titanium (Ti), with set defined materialistic properties of mass density, Poisson's ratio, Young's modulus, and Yield Strength of 4600 kg/m³, 0.3, 1.1E11 Pa and 1.4E8 Pa respectively, along with a wall thickness of 260 mm. Table 4 displays the parameters for the interface ring at varying boundary conditions for the figure number from the reports obtained from the FEA simulation.

Table 4: Parameter values for Interface Ring FEA analysis

Figure Number	Ocean Depth (m)	Water Pressure (kPa)	Maximum Von Mises Stress (Pa)	Factor of Safety (FOS)
16	3800	38144.73	6.24E7	2.24
17	8768.76	88000	1.44E8	0.97

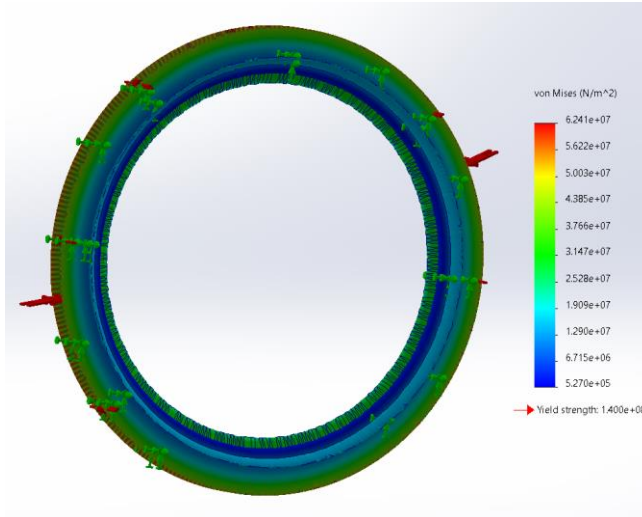


Figure 16: Interface Ring at a depth of 3800 m

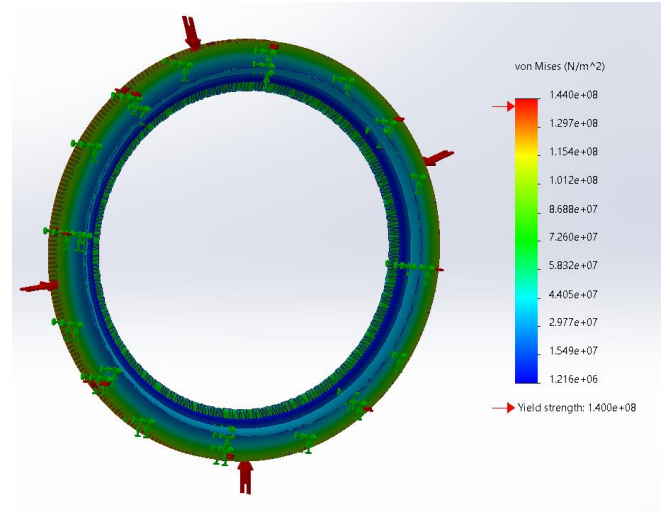


Figure 17: Interface Ring at a depth of 8768.76 m

From the tabulated results in table 4, at the ocean depth of 3800 m, at the Titanic depth, the interface rings of the Titan had a factor of safety of 2.24. Figure 17 exhibits the stress acting on the edges of the ring where it possibly might lead to structural failure. In addition, it can be seen that at a depth of 8768.76 m, the interface ring of the Titan begins to weaken in its structural strength and ends up failing.

4.2 Computational Fluid Dynamics (CFD) Analysis

Simplifying the geometry to a symmetrical shape enabled us to only perform simulations for two scenarios instead of four.

4.2.1 CFD Analysis in XY-axis

Figure 18(i) and 18(ii) shows the mesh configuration for the part domain for the CFD analysis in the xy-axis plane. Figure 20 to Figure 25 (see appendix) investigate the effects of water pressure acting on the max pressure and max velocity at various depths. The maximum pressure peaks early during the analysis whereas the maximum velocity is a slow increase for all the depths. Figure 26 to Figure 31 (see appendix) shows the pressure and velocity gradient for the CFD analysis in the xy-axis.

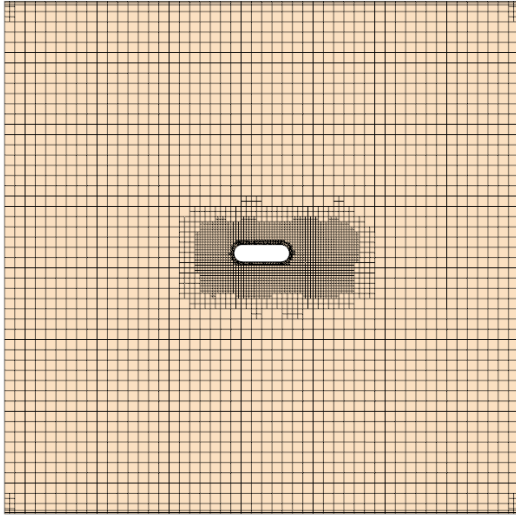


Figure 18(i): Mesh configuration of the part in *xy*-axis

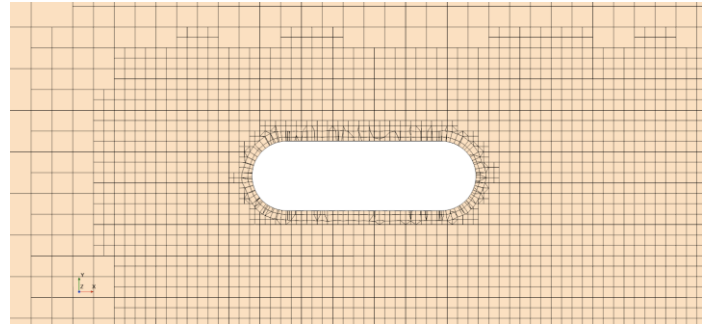


Figure 18(ii): Mesh configuration of the part in *xy*-axis (zoomed in)

4.2.2 CFD YZ-axis analysis

Figure 19 shows the mesh configuration for the part domain for the CFD analysis in the *yz*-axis plane. Figure 32 to Figure 37 (see appendix) investigates the effects of water pressure acting on the max pressure and max velocity at various depths. The maximum pressure peaks early when at sea level but when at a deeper depth, the maximum pressure plateaus before plummeting to nearly zero, whereas the maximum velocity slowly increases at sea level and deeper depths, the velocity peaks before becoming constant. Figure 38 to Figure 43 (see appendix) shows the pressure and velocity gradient for the CFD analysis in the *yz*-axis.

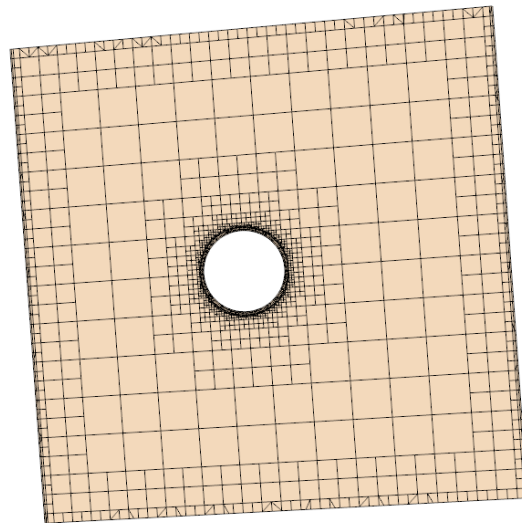


Figure 19: Mesh configuration of the part in *yz*-axis

With the mesher parameters such as prism layer near wall thickness at 0.001 m, prism layer total thickness of 33.33 relative to base, target surface size 10 relative to base, minimum surface size 10 relative to base and number of prism layers of 2 were kept constant, multiple simulations were executed on the design to demonstrate the mesh independence with the CFD simulation in Star CCM+. With the increase in base size, while keeping other variables constant, the max. velocity and max. Pressure differences were investigated.

From Table 5 it can be deduced that with the increase in mesh element count, there was no significant change in the max. velocity or max. pressure. Furthermore, due to the limited computational processing power of the device, the information for the base size of 0.05 m could not be determined. Therefore, it can be concluded that CFD simulation was independent of the mesh size.

Table 5: Mesh independency at 3800m

Base size (m)	Mesh element count	Max Velocity (m/s)	Max Pressure (Pa)
1.0	293763	2.30	3.15E7
0.5	1102372	2.29996	3.15E7
0.25	4483234	2.29973	3.15E7
0.05	Could not process	Could not process	Could not process

5.0 Summary and Conclusion

In conclusion, our multidisciplinary approach that combines Computational Fluid Dynamics (CFD) and Finite Element Analysis (FEA) has yielded different perspectives into the engineering complexities of the Titan submarine. With a factor of safety of 3.22 of the hull, 4.32 of the backward end cap, 3.59 of the forward end cap, and 2.24 of the rings, the achievable depth of the Titan would be 3800 m without structural failure. However, the hull showed evidence of structural degradation at an extreme depth of 12348 meters, highlighting how crucial it is to recognize the limitations in the vessel's design. FEA simulations provided a thorough understanding of stress distribution and possible failure situations by studying the structural integrity of individual components. However, CFD simulations in the XY and YZ axes offered important information about hydrodynamic resistance behavior, which is important for stability and maneuverability.

The results were further backed by the mesh independence analysis in CFD, which showed that mesh size did not influence our simulations. The challenges arise from complex factors like pressure, material properties, and turbulent fluxes along with some degree of uncertainty because the simulation assumptions may not accurately reflect real-life events, even if they are necessary for simplification. Furthermore, there could be unforeseen challenges when implementing our idea in the harsh deep-sea environment.

6.0 Contribution Statements

Contributor	Contribution
Mohammad Ebrahimi	Part design, CFD Analysis
Muhammad Farhan	Part design, FEA Simulations
Azwad Hammad	Part design, Report, Part Optimization

7.0 References

- [1] MatWeb. "Material Data Sheet," MatWeb,
https://www.matweb.com/search/datasheet_print.aspx?matguid=39e40851fc164b6c9bda29d798bf3726.
[Accessed: Dec 07, 2023].
- [2] M. Belof, "Composite submersibles under pressure in deep, deep waters," CompositesWorld, Available:
<https://www.compositesworld.com/articles/composite-submersibles-under-pressure-in-deep-deep-waters>.
[Accessed: Dec 07, 2023]

Appendix

CFD Analysis in XY-axis

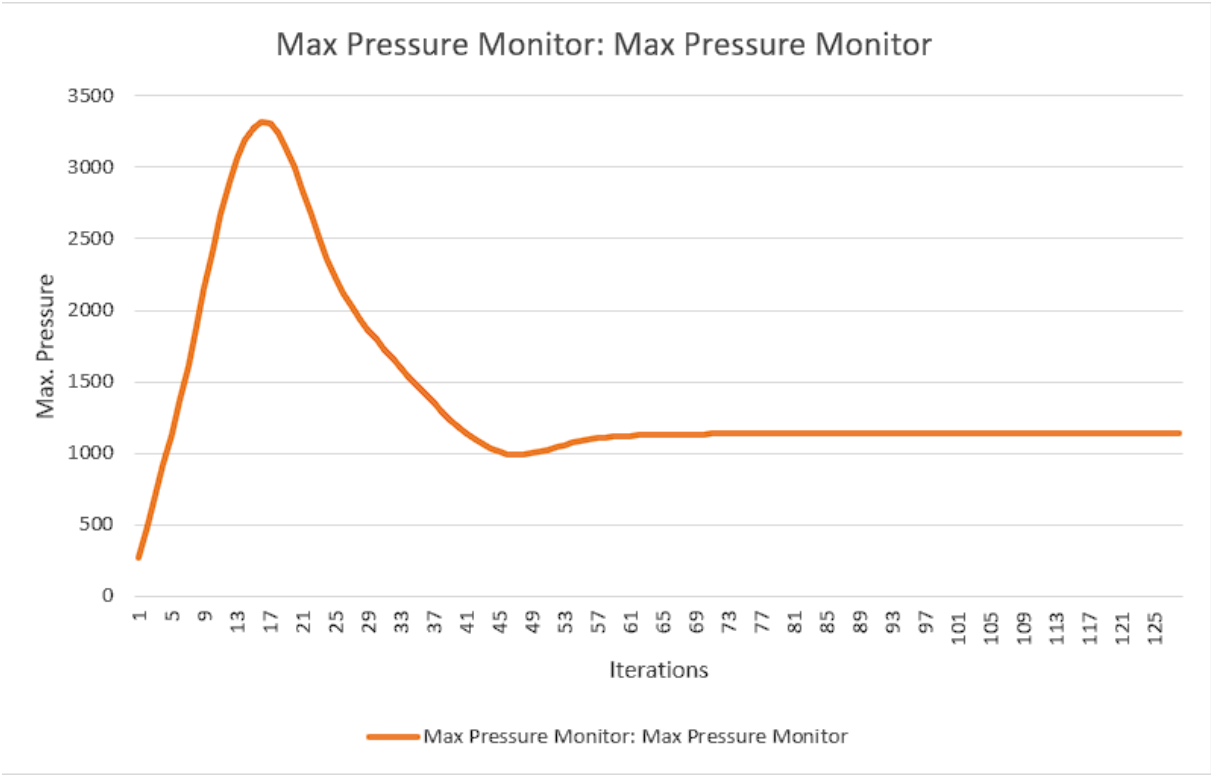


Figure 20: Max pressure at 0 m

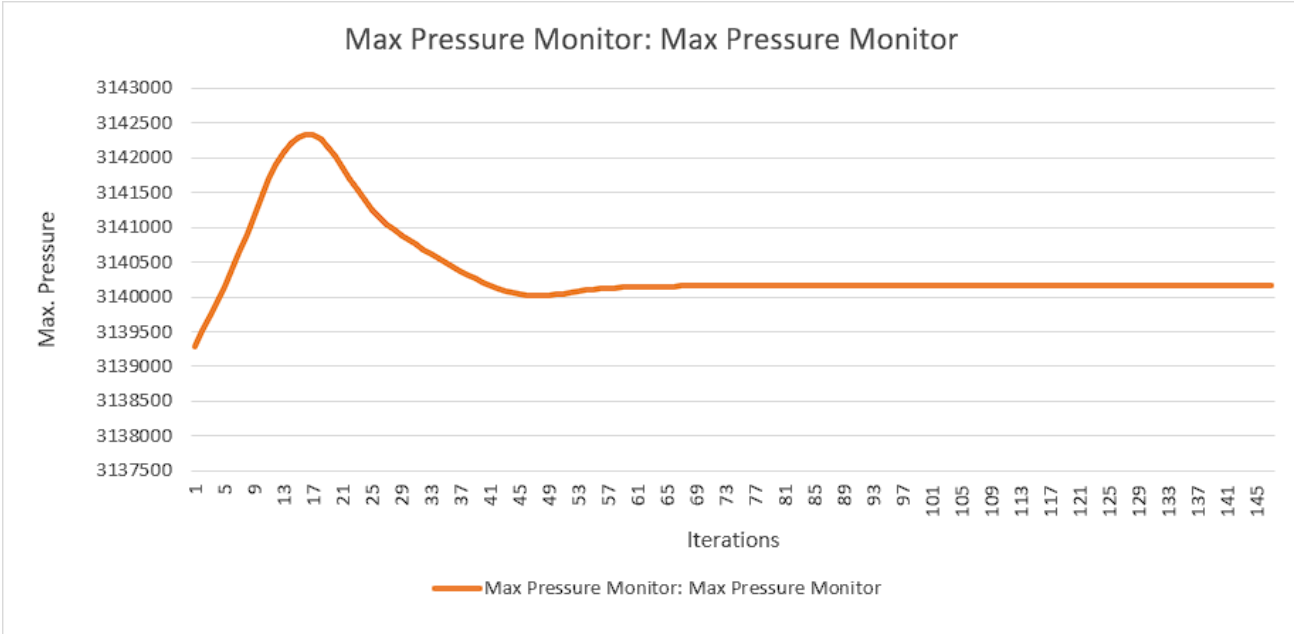


Figure 21: Max pressure at 4000 m

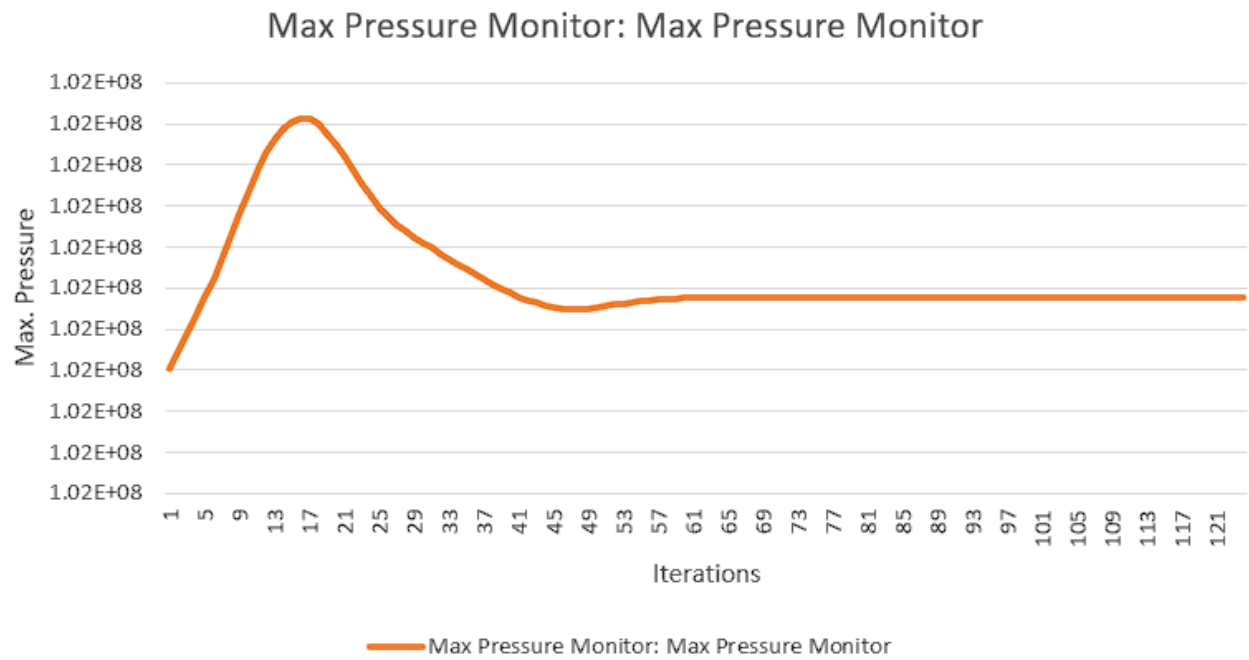


Figure 22: Max pressure at 12000 m

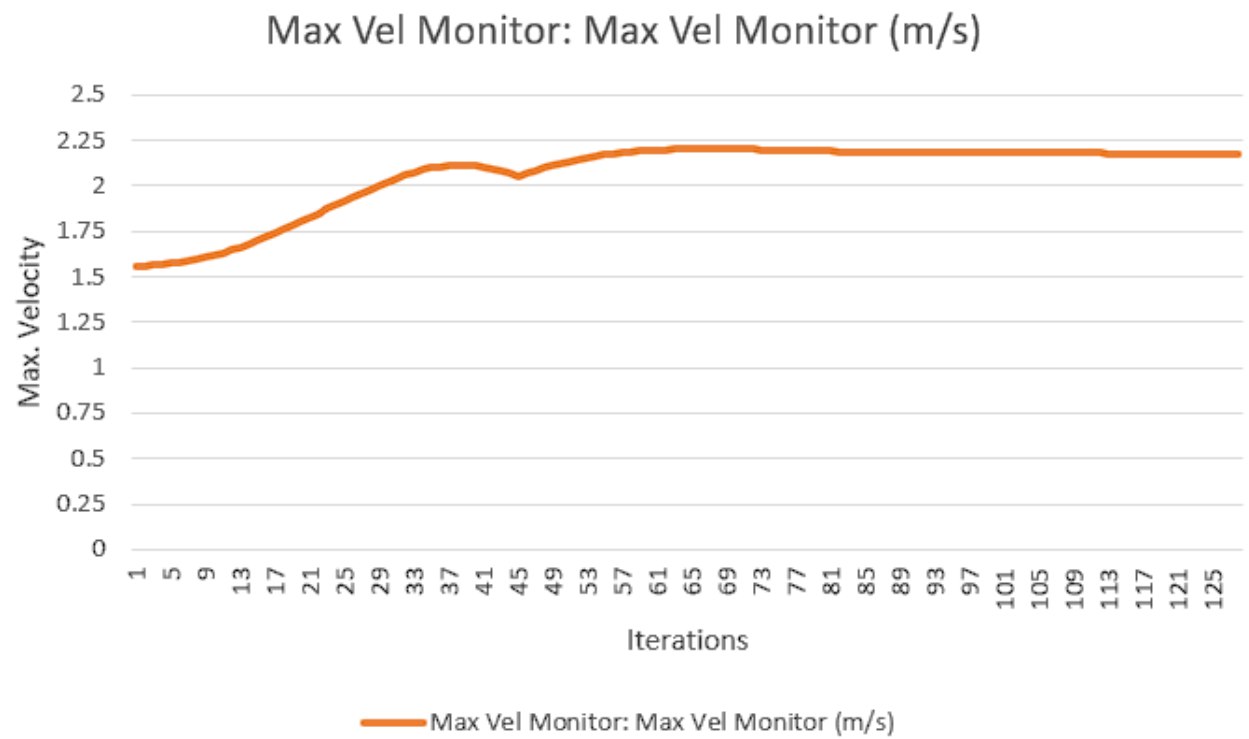


Figure 23: Max velocity at 0 m

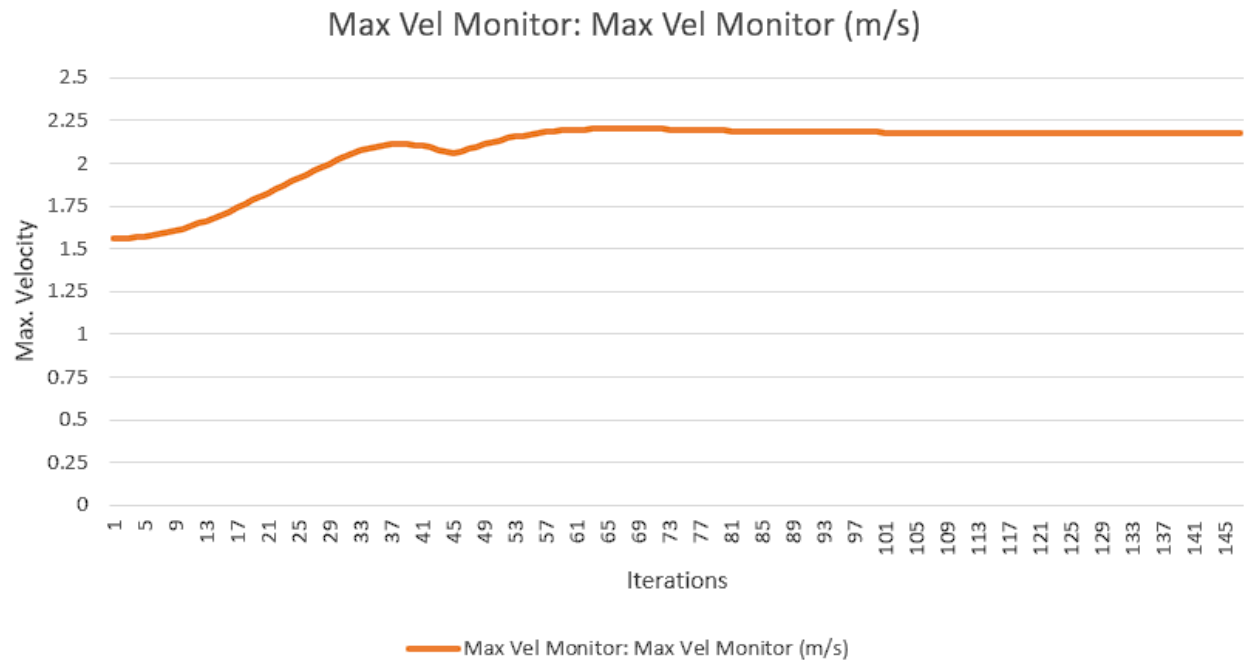


Figure 24: Max velocity at 4000 m

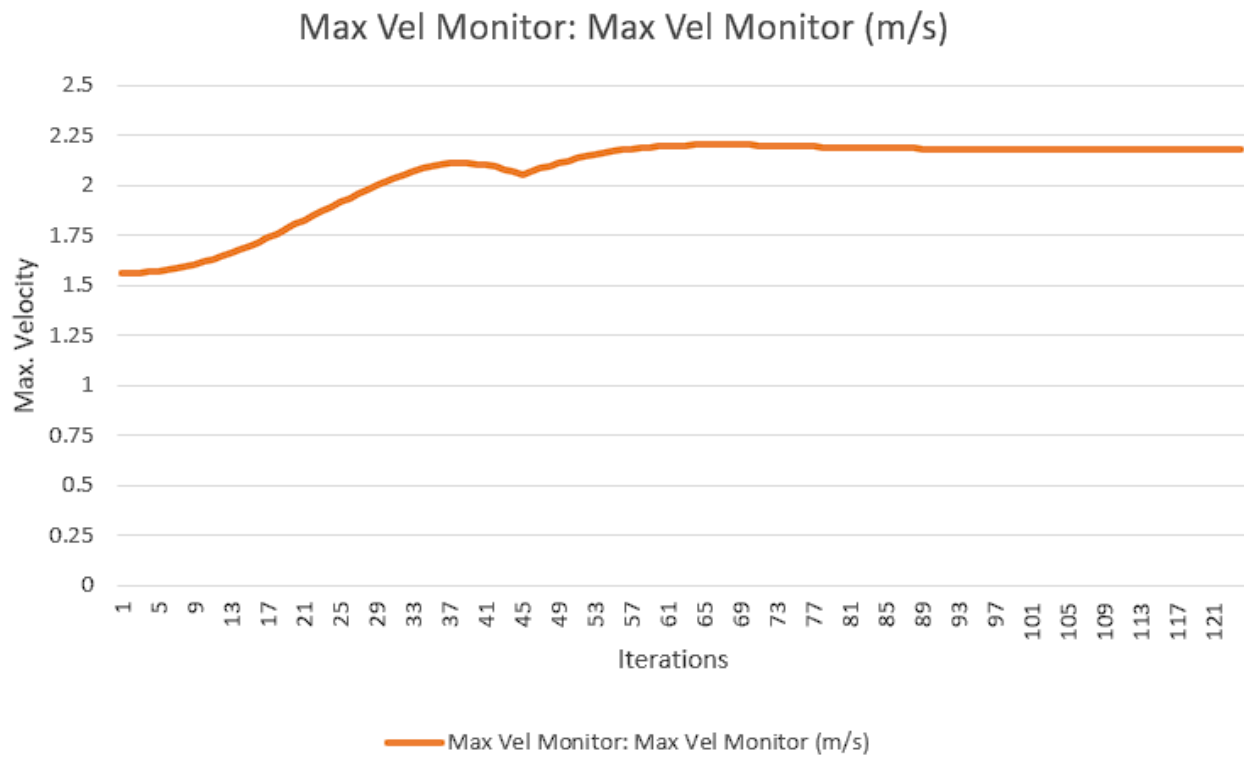


Figure 25: Max velocity at 12000 m

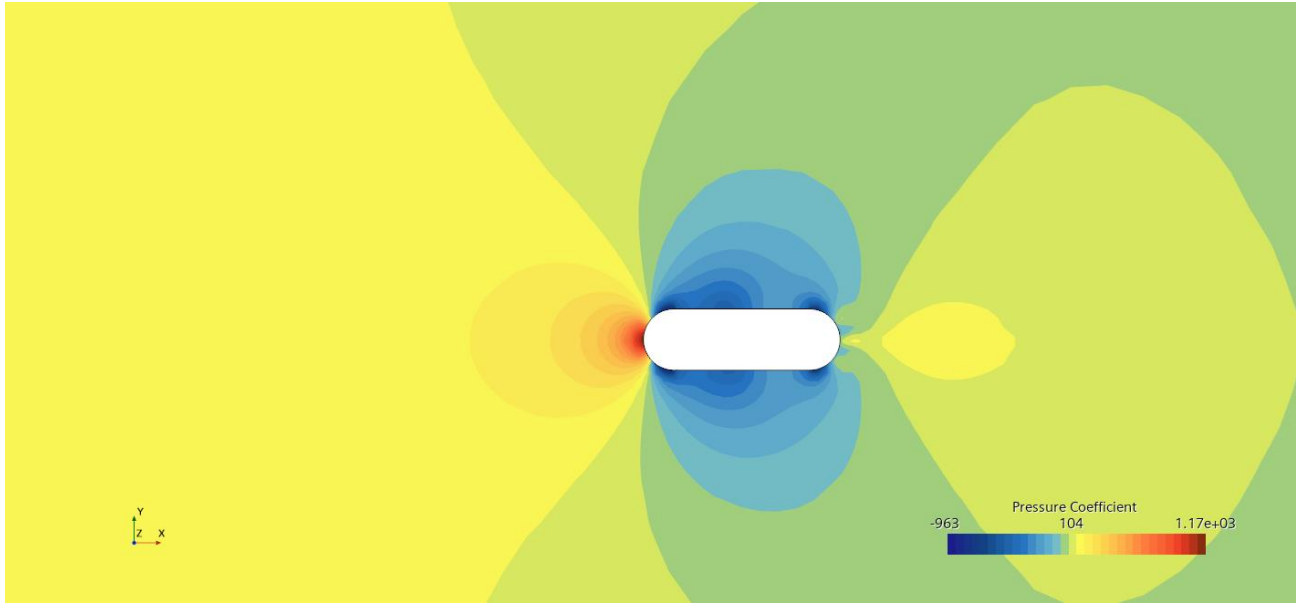


Figure 26: Pressure at 0 m

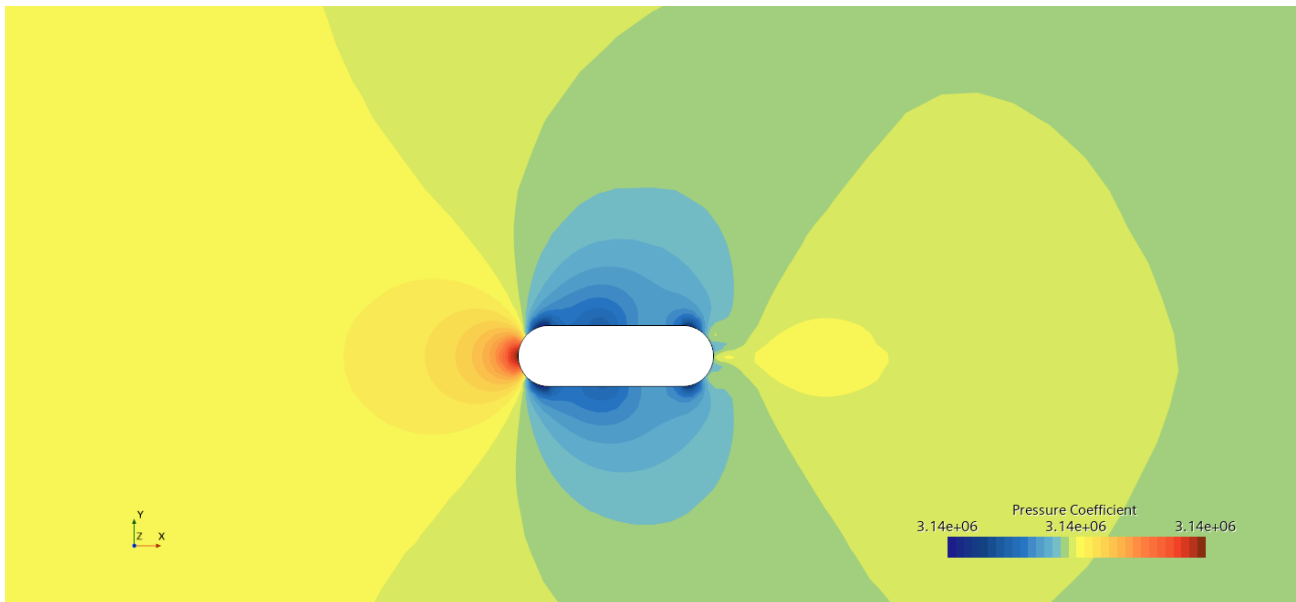


Figure 27: Pressure at 4000 m

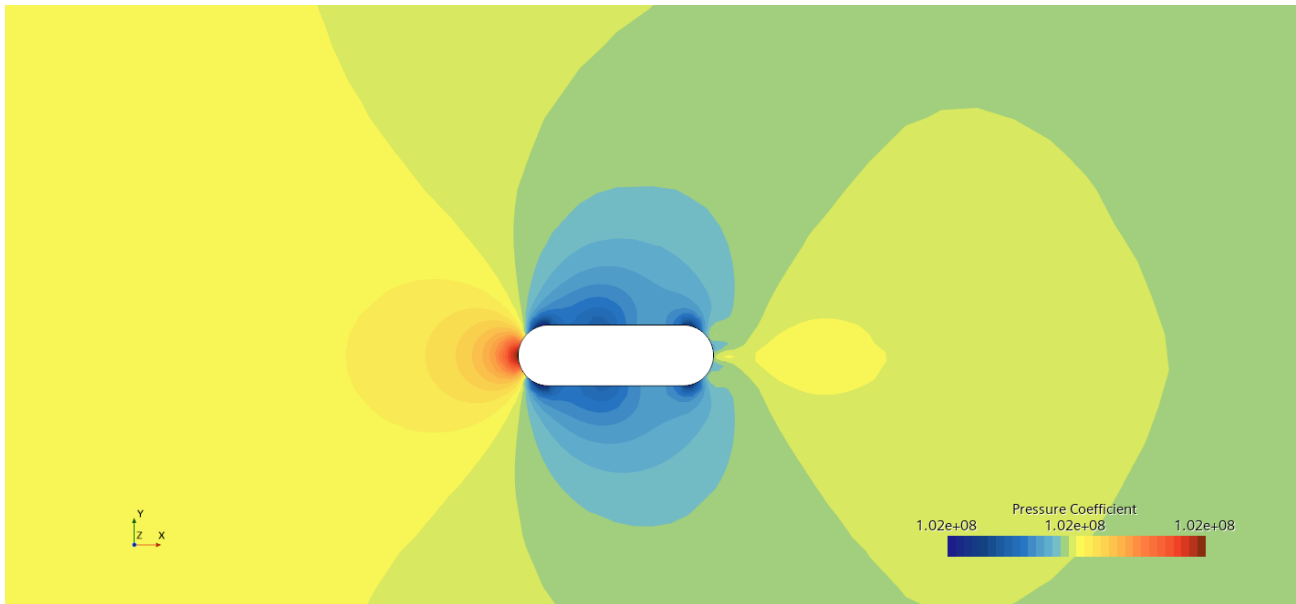


Figure 28: Pressure at 12000 m

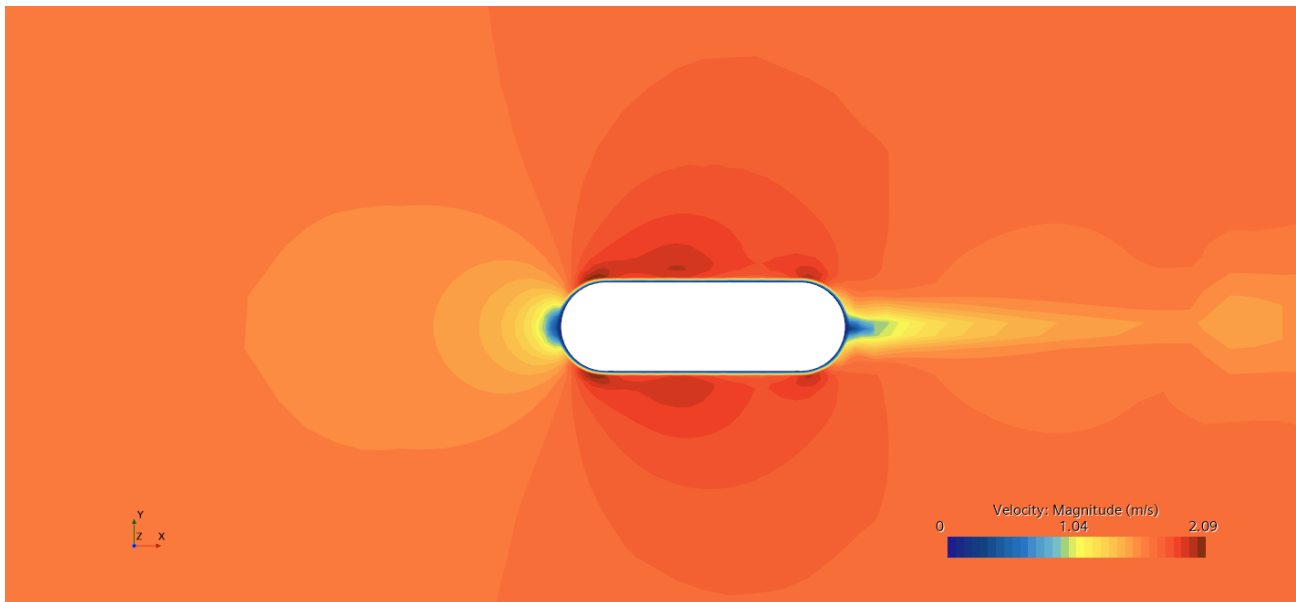


Figure 29: Velocity at 0 m

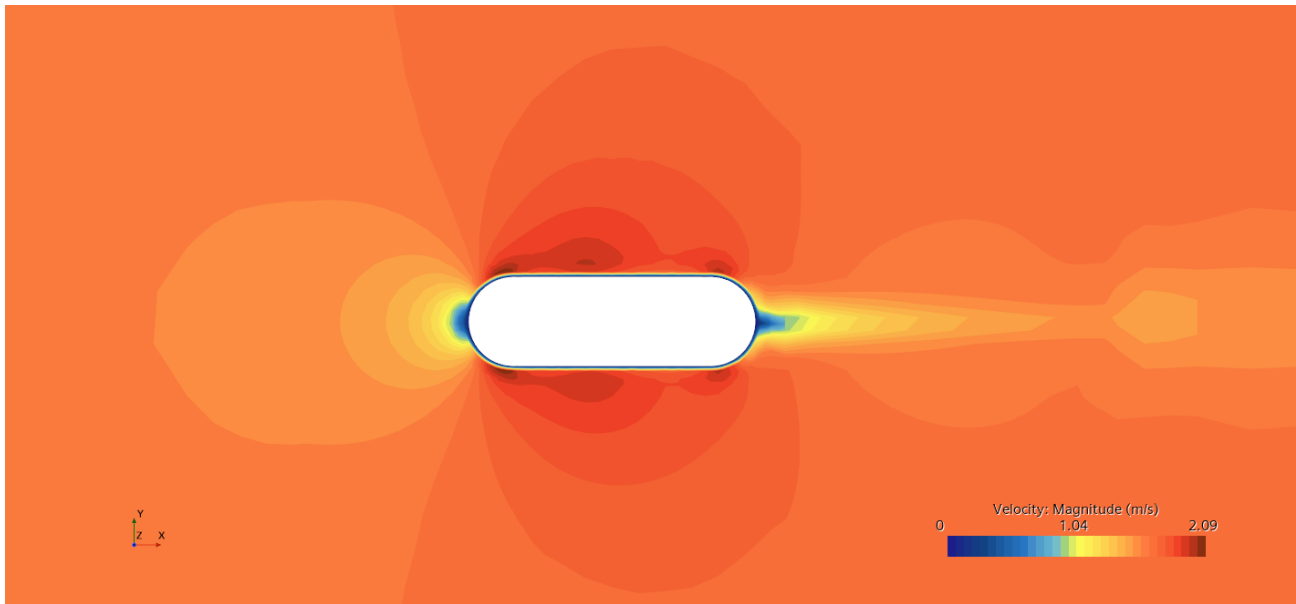


Figure 30: Velocity at 4000 m

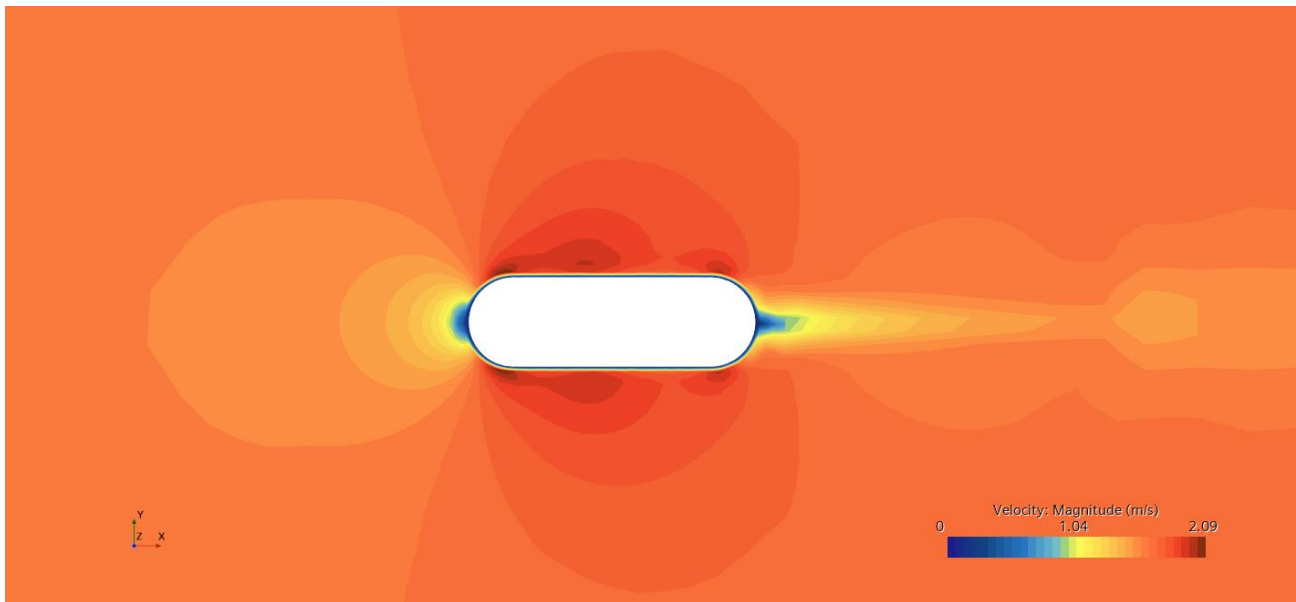


Figure 31: Velocity at 12000 m

CFD YZ-axis analysis

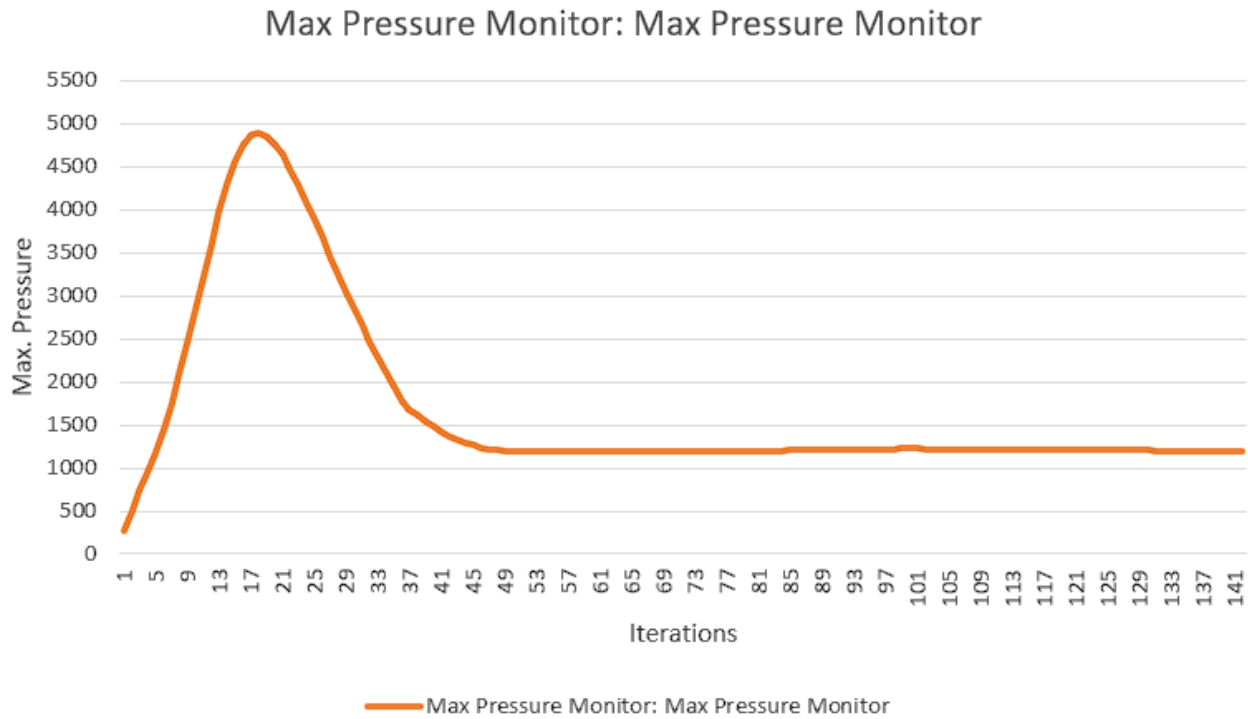


Figure 32: Max pressure at 0 m

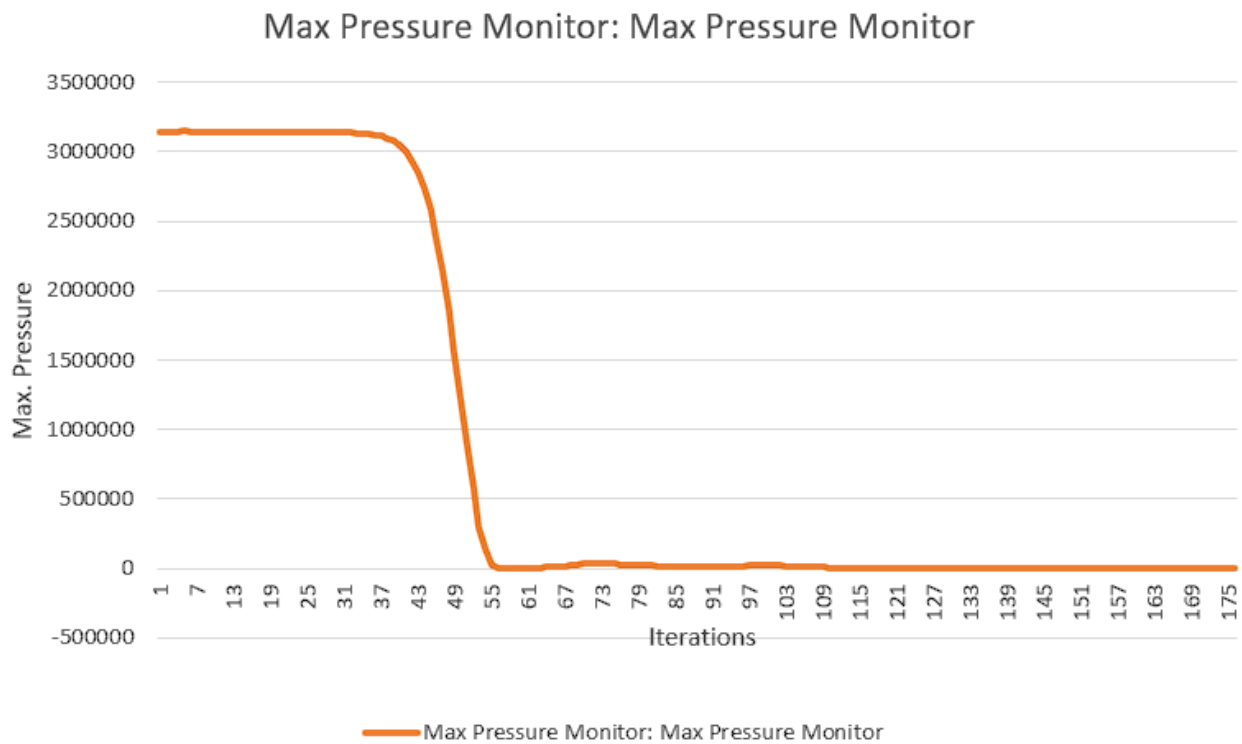


Figure 33: Max pressure at 4000 m

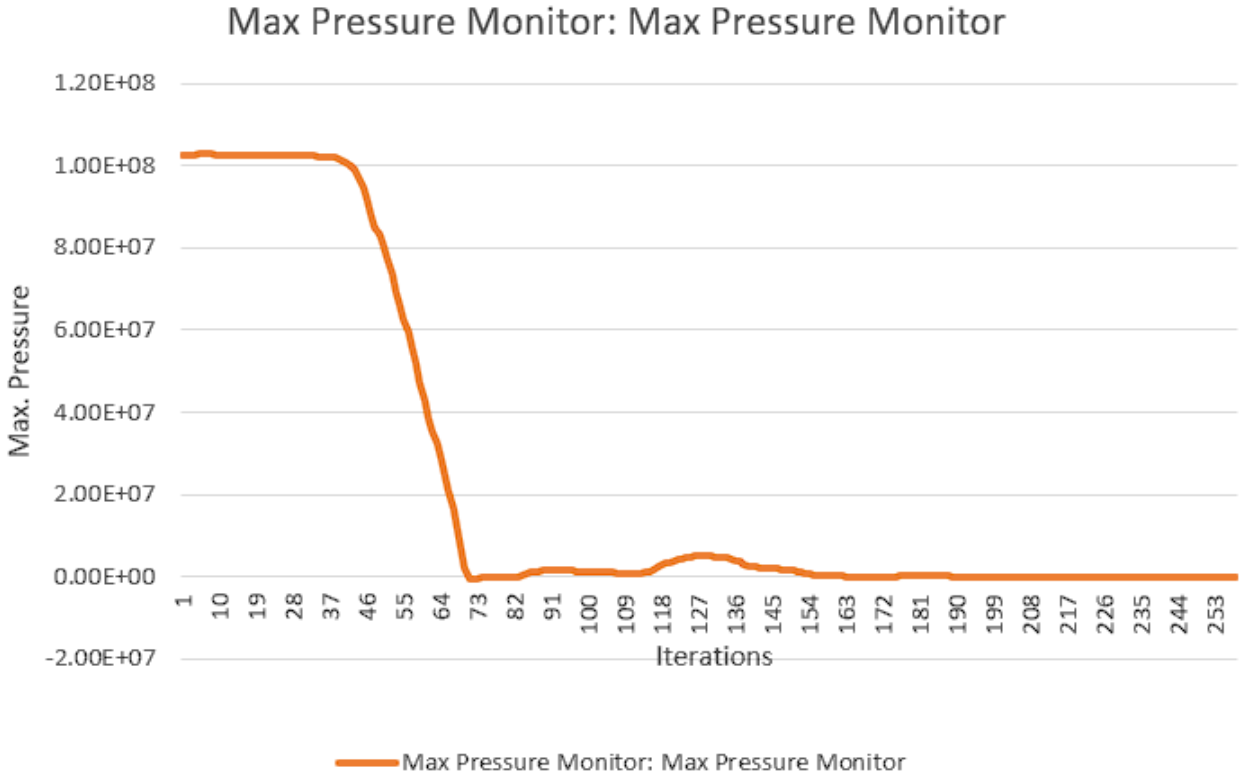


Figure 34: Max pressure at 12000 m

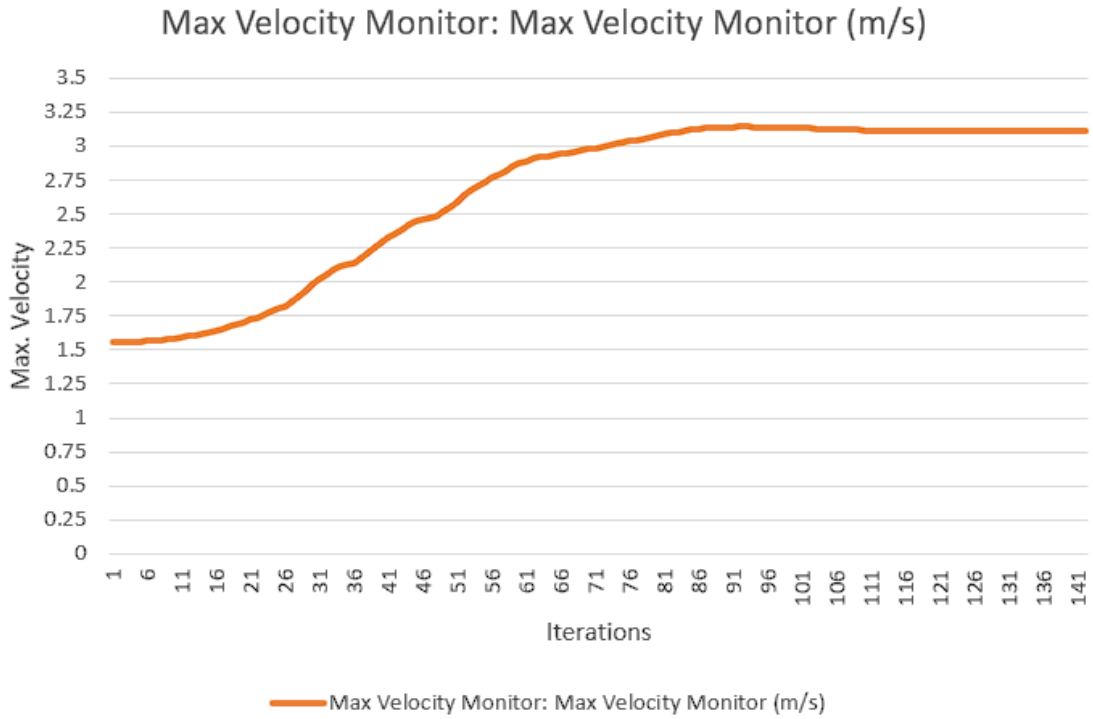


Figure 35: Max velocity at 0 m

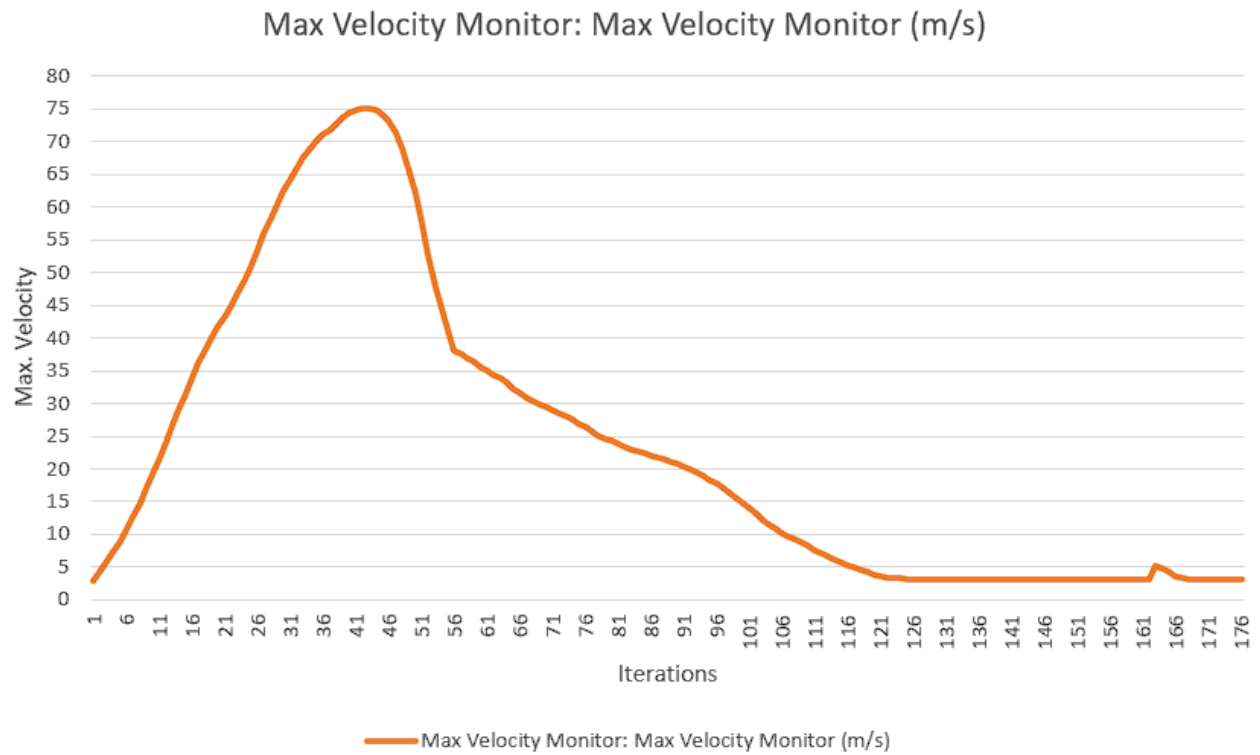


Figure 36: Max velocity at 4000 m

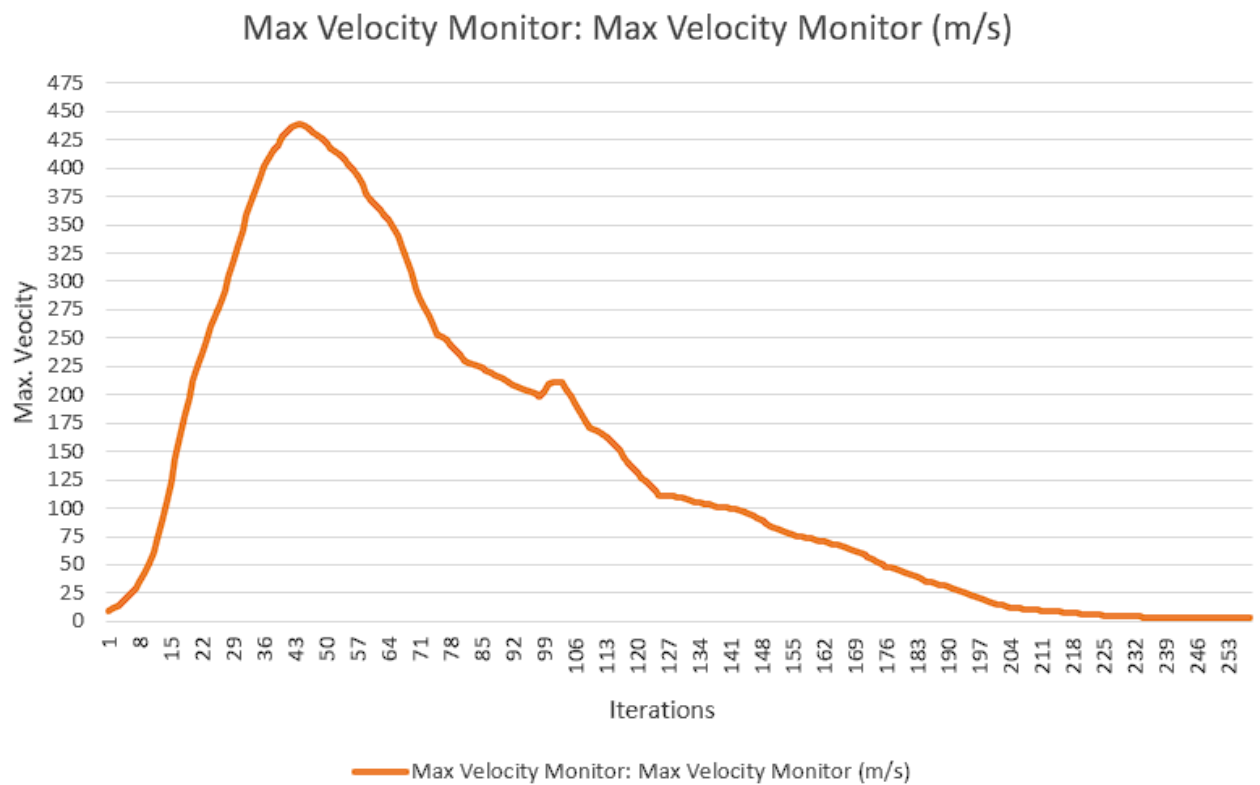


Figure 37: Max velocity at 12000 m

Simd

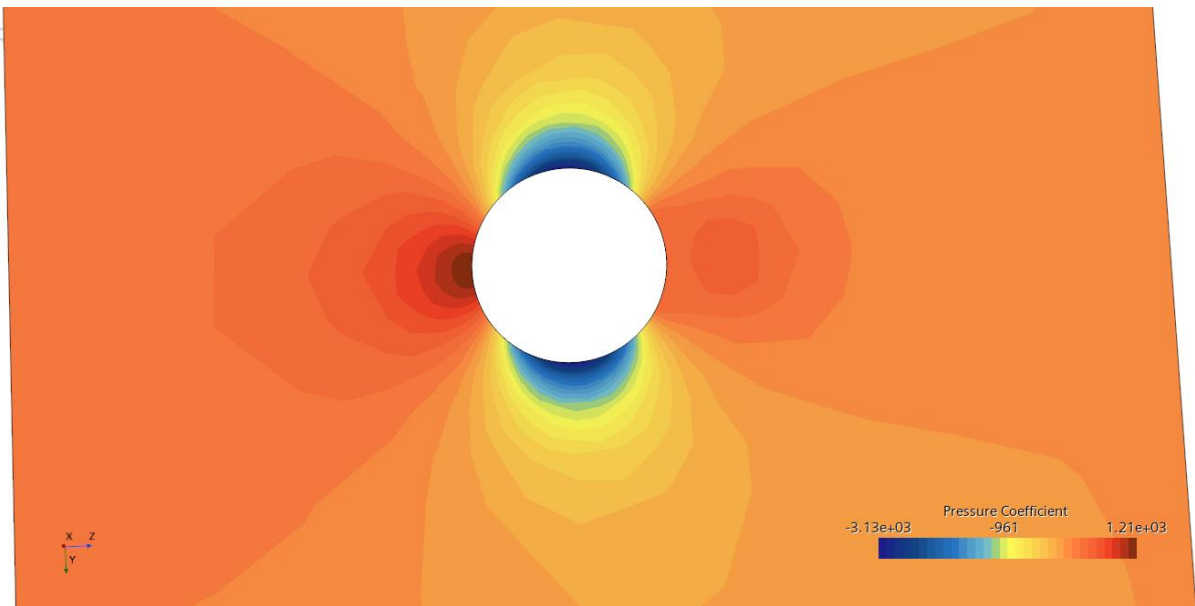


Figure 38: Pressure at 0 m

Simd

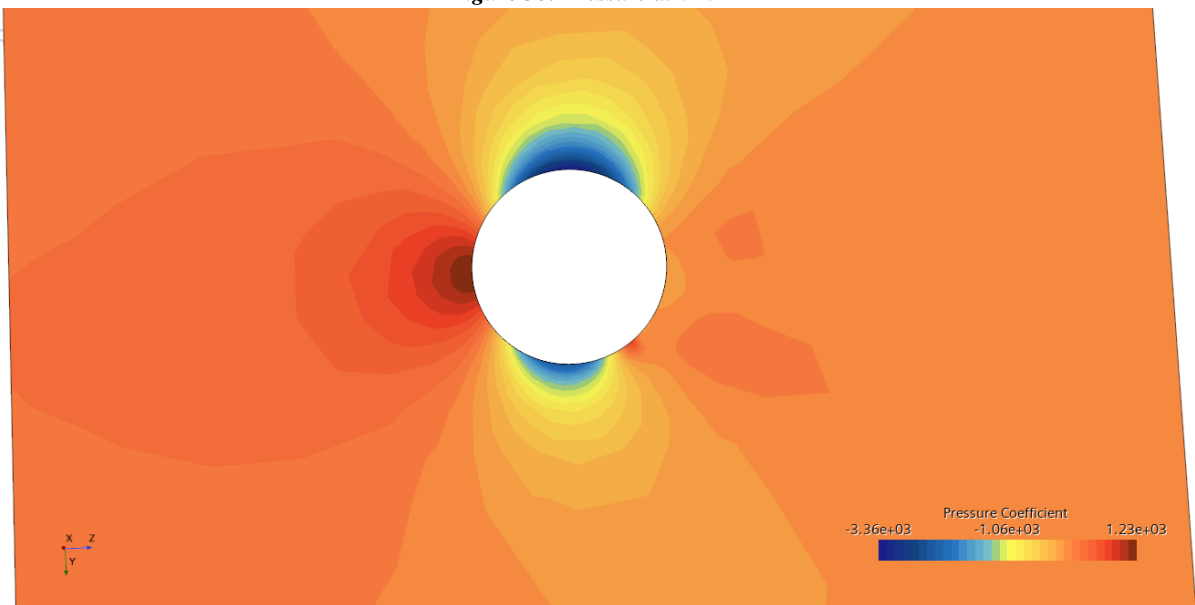


Figure 39: Pressure at 4000 m

Sim

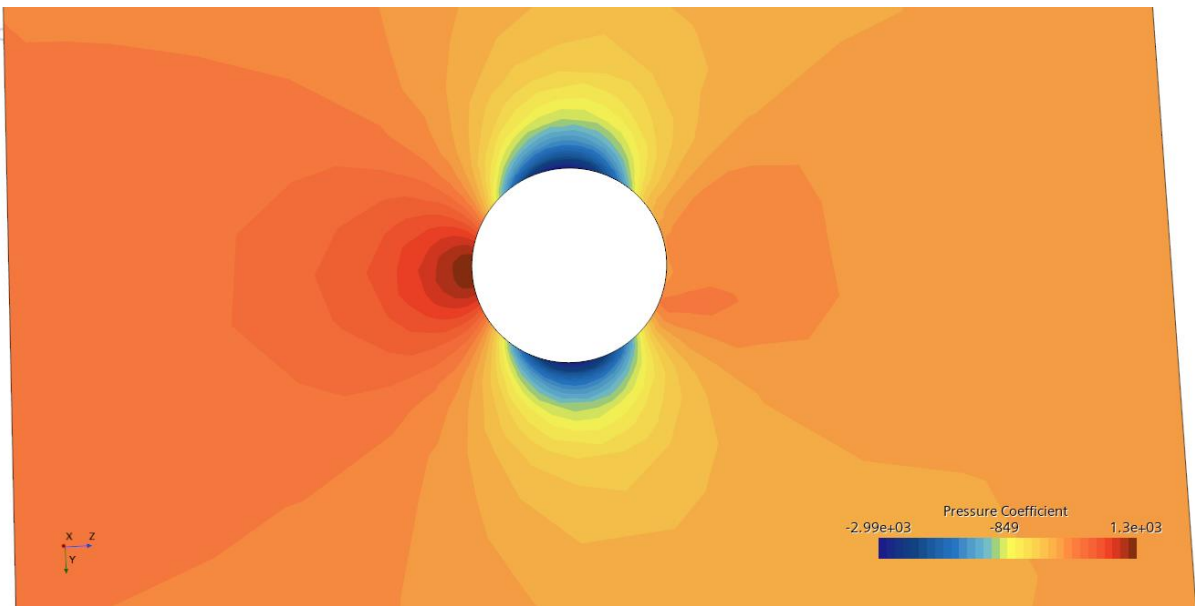


Figure 40: Pressure at 12000 m

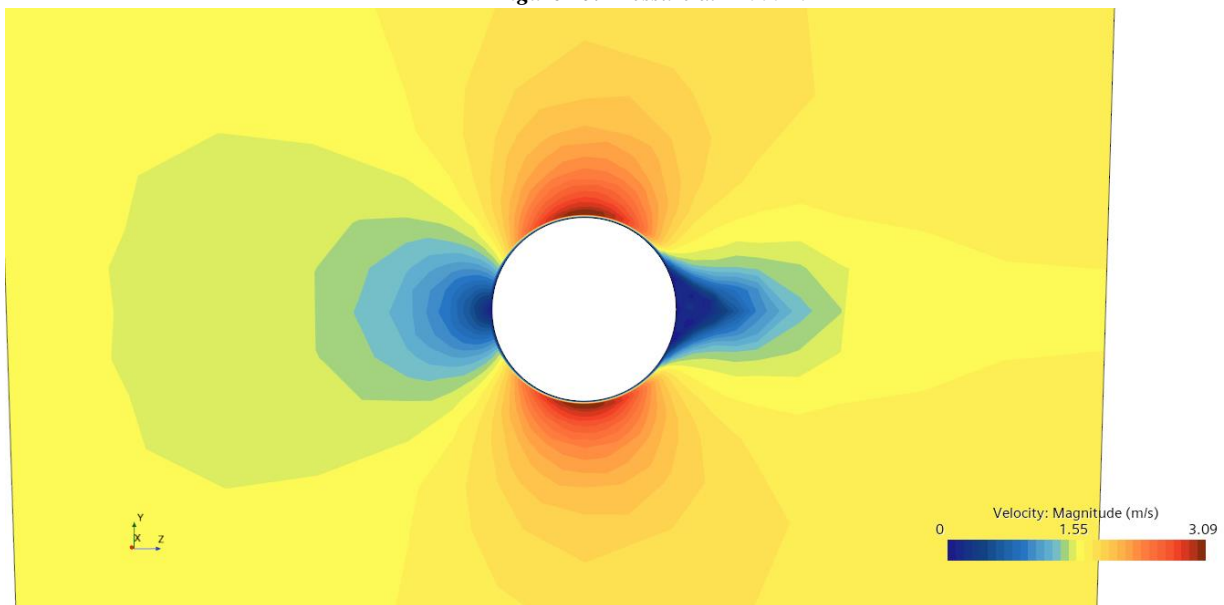


Figure 41: Velocity at 0 m

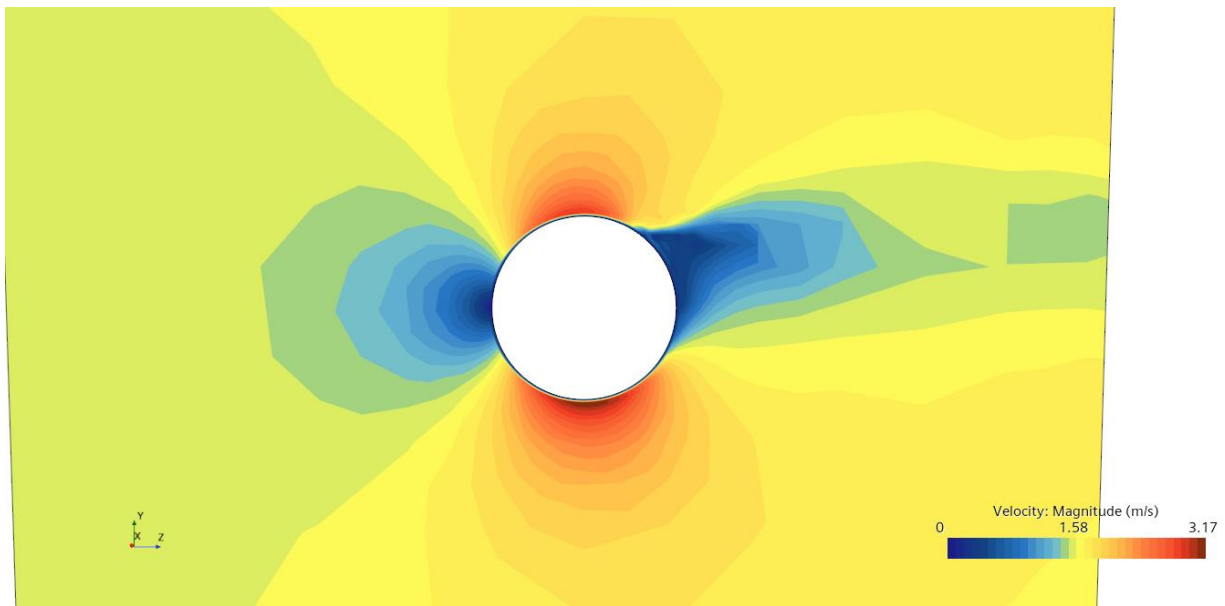


Figure 42: Velocity at 4000 m

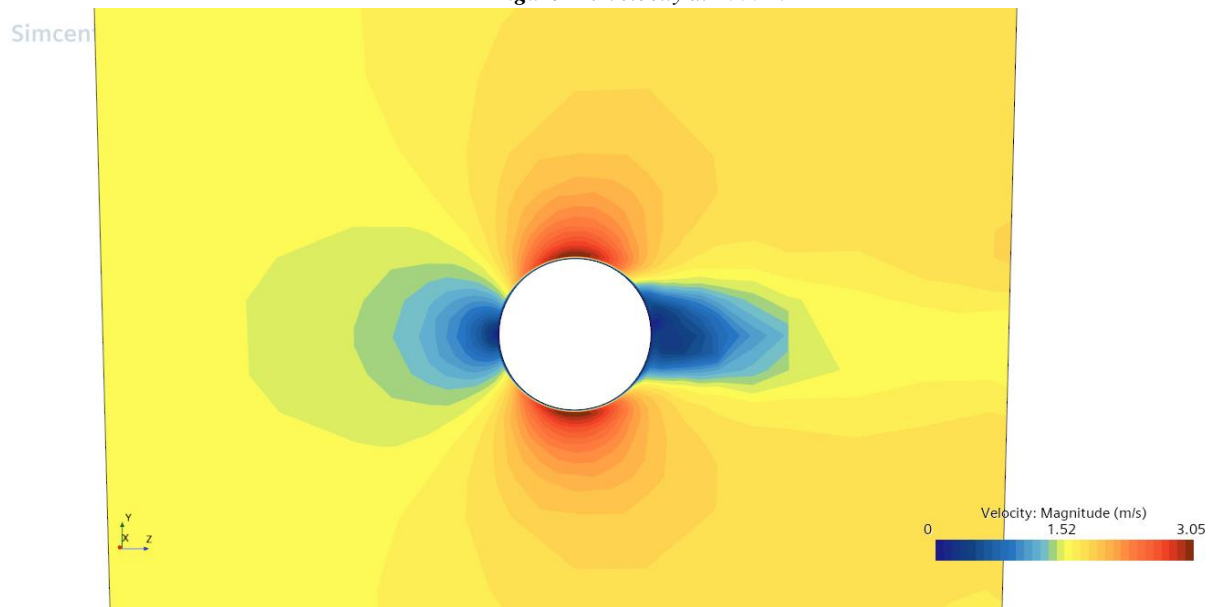


Figure 43: Velocity at 12000 m